Core-polarization-corrected random-phase approximation with exact exchange for dipole surface plasmons in silver clusters

Fengyuan Xuan* and Claude Guet†

Energy Research Institute at Nanyang Technological University (ERI@N), 1 Clean Tech Loop, Clean Tech One, Singapore 637141

(Received 19 August 2016; published 20 October 2016)

The surface plasmon in silver clusters is red shifted with respect to standard jellium random-phase approximation (RPA) predictions that work well for simple metal clusters. The reason for the deviation arises primarily from the non-negligible polarization interaction between the valence electrons and ionic cores. In order to quantify this effect in the jellium approximation we introduce a modified RPAE (RPA with exact exchange). The jellium background of Ag cores is treated as a polarizable sphere. This model predicts a dipole surface resonance in excellent agreement with published experimental data. Moreover it yields the blue shift (red shift) with decreasing sizes for cationic (anionic) Ag clusters as observed experimentally.

DOI: 10.1103/PhysRevA.94.043415

I. INTRODUCTION

Quantum confinement in simple metallic nanoclusters leads to an electronic shell filling similar to those of atoms or nuclei, as evidenced in the historical mass-spectra experiment by Knight [1], which showed that sodium atoms tend to aggregate with magic numbers ($N = 8$, 20, 40, 58, 92, ...). Following this discovery, much attention has been paid to alkali-metal clusters, both experimentally and theoretically. In particular optical absorption has been carefully studied as it reveals collective dipole modes referred to as surface plasmon [2–10]. It is settled that the optical properties of small sodium clusters with a magic number of valence electrons can be understood as the quantum collective response of these electrons in an ionic background which is approximated by a uniformly charged sphere (jellium model [11–13]). Although the ionic structure is completely neglected, the random-phase approximation (RPA) description of this collective motion reproduces the position of the surface plasmon and its red shift as the cluster size decreases. Because the confining external potential deviates from a harmonic oscillator potential only outside the jellium core, one can appeal to the Kohn theorem for a zeroth-order estimate. The Kohn theorem states that for a system with interacting particles in a confining external harmonic oscillator potential, a single state contains the whole dipole strength [14,15]. The frequency of this collective mode is equal to that of the confining potential, independently of the interaction among the particles and of the number of particles. The electron-ion potential inside the jellium sphere is a harmonic oscillator with a frequency given by

$$\omega_{\mathrm{ho}}^2 = \frac{e^2}{4\pi\epsilon_0 m_e r_{\mathrm{S}}^3}, \tag{1}$$

where r_{S} is the Wigner-Seitz radius. The measured red shift is due to the finite size, through two separate mechanisms. One is associated with the deviation of the electron-ion potential outside the jellium sphere from the harmonic potential while the other one is associated with a many-body effect which couples the center of mass of motion and the intrinsic electron motions [16]. Note that there is a close connection between these two contributions since both effects arise from the spill-out electrons.

The RPA in the jellium model approximation captures the main features of the collective dipole mode of simple metal clusters. However, it works well only for sodium and potassium clusters and fails to predict correctly the optical response of lithium clusters. Nevertheless a good agreement between the measured giant dipole resonance and a modified jellium model could be achieved by correcting the electron-ion potential by adding a nonlocal angular-momentum-dependent potential that accounts for the expected fundamental difference between s-wave and p-wave scattering by the lithium core which has only s-core electrons. Within this physically sound and relatively simple modification the theory could not only predict the observed position but also explain the experimentally reduced observed optical strength and yield a correct effective mass due to the nonlocality of the background potential [17].

Can silver clusters with delocalized $5s$-valence electrons be reasonably well described within a jellium RPA approach? Optical properties of quantum-sized silver clusters have been studied extensively and general trends have emerged. Treating a silver cluster as a classical dielectric sphere, the optical absorption cross section in the long wavelength can be written as

$$\sigma(\omega) = \frac{4\pi\omega R^3}{c}\mathrm{Im}\frac{\epsilon(\omega)-1}{\epsilon(\omega)+2}. \tag{2}$$

Inserting empirical bulk values of the dielectric function into the above formula, one predicts a peak at 3.5 eV, which is much lower than the value of 5.2 eV given by Eq. (1). In the case of sodium, both values would agree, reflecting the fact that sodium is well described in the Drude model. The deviation between both values in the case of silver indicates that it is no longer justified to neglect the polarization of other electrons, namely, the filled d shell [18].

In the early nineties, Tiggesbäumker *et al.* published a set of photodepletion spectroscopy experiments which showed that the absorption spectrum of Ag cationic clusters has a blue shift from 3.8 to 4.4 eV as the number of atoms in cluster decreases from 70 to 5 [19,20]. These authors also provided a phenomenological model that explained that the observed shift was due to a reduced s-d screening interaction in the surface

*Interdisciplinary Graduate School, Nanyang Technological University, Singapore.

†Corresponding author: cguet@ntu.edu.sg

region. Later, Tiggesbäumker *et al.* conducted the same type of measurements for small negatively charged silver clusters [21] and observed a red shift with decreasing size which they could explain within the framework of the phenomenological model used to account for the blue shift associated with cationic clusters. The role of d electrons and the observed blue and red shifts have also been discussed in the framework of a two-region model by several authors [22,23].

On the theory side, a generalized time-dependent density functional theory (TDDFT) was proposed by Serra and Rubio to treat the effects of polarization of ionic cores on the optical response of silver clusters [24]. This model was a finite system extension of the work of Zaremba *et al.* [25,26]. As the induced valence electron density polarizes the ionic cores, mainly the $4d$ electrons, the effective potential felt by the valence electrons includes a dipole core-polarization potential. Meanwhile, from a pure theoretical point of view, atomic packing symmetry effects on the absorption spectrum of silver clusters were studied by TDDFT calculation with an 11-electron pseudopotential, and different exchange correlation functionals were tested for use in TDDFT calculations [27–29].

The RPA response of a finite electron system to a weak oscillating dipole field goes beyond the independent particle response by adding consistently to the external potential the potential that is induced by the density fluctuations. The RPA can be formulated within two different representations. In the time-dependent local-density approximation (TDLDA) the density change is the key parameter and one solves the self-consistent equation for the susceptibility [30–34] whereas in the matrix formulation the configuration space is that of the single orbitals [35]. The two methods are physically equivalent. However, the TDLDA approach does not allow one to treat a nonlocal exchange interaction but rather any interaction which is the sum of the direct Coulomb interaction and any local interaction deriving from a density-dependent potential. The RPAE (RPA with exact exchange), which accounts for the nonlocal exchange interaction, is thus necessarily formulated in the matrix form, the residual two-body interaction from Hartree-Fock (HF) theory being diagonalized in the space of one-particle–one-hole excitations [36,37]. Matrix RPA and TDLDA were compared numerically and shown to give similar optical properties for Na clusters [38].

The present theoretical work treats the mutual interaction between core- and valence-electron fluctuations within the matrix formulation of RPAE. The model space is therefore the Hartree-Fock model for the valence electrons with a two-body interaction made of two contributions, namely, the usual Coulomb interaction and the dipole core-polarization interaction. The core-polarization interaction also generates a one-body dipole polarization potential which adds to the jellium Coulomb potential. The dipole vibrational modes are readily obtained by solving the RPAE matrix equation, with matrix elements of the core-polarization-modified residual interaction between particle-hole excitations on one block and ground-state and two-particle–two-hole interactions on the other block; all these terms have a direct and an exchange part. This approach differs from that of Ref. [24] by capturing immediately at the level of the model space the exchange interaction exactly, both in the Coulomb and the core-polarization terms. As in Ref. [24], the input parameter is the dipole polarizability of the Ag^+ ions. Whereas a free ion polarizability value is assigned to ions lying on the surface of the cluster, an estimated embedded polarizability value is assigned to ions lying inside the cluster. Within these assumptions Serra and Rubio explained the blue shift of the plasmon peak with decreasing size by an increasing percentage of surface Ag^+ ions with free ion polarizability. We shall see in our model that the one-body attractive polarization potential also contributes to the blue shift.

As has been discussed before, a pure jellium model fails to predict the optical spectra of small Ag clusters. However, we would like to keep the simplicity of the jellium model and extend it to understand the s-d electron interaction in Ag clusters. In the following section, we present a core-polarization-corrected RPAE jellium model. Numerical calculations are done for anionic, neutral, and cationic silver clusters with closed-shell number of electrons (8, 20, 58, 92, 138, 198). The effects of the one-body and two-body terms on the shift of oscillator strength will be discussed. Comparison of our calculations with experiment will be given and good agreement is found. An atomic system of units ($\hbar = e = m_e = 4\pi\epsilon_0 = 1$) is used throughout the paper.

II. CORE-POLARIZATION-MODIFIED RPAE FOR JELLIUM SILVER CLUSTERS

In the simple jellium model, a closed-shell neutral cluster of N simple metal atoms is treated as a system of N electrons (one valence electron per atom) confined by a uniformly charged spherical background. The Hamiltonian for this N-electron system is given by

$$H = \sum_i \left(-\frac{1}{2}\nabla_i^2\right) + \sum_i V_{\rm JM}(\mathbf{r}_i) + \sum_{i<j} \frac{1}{|\mathbf{r}_i - \mathbf{r}_j|}, \qquad (3)$$

where

$$V_{\rm JM}(r) = \begin{cases} -\frac{N}{2R_J}\left(3 - \left(\frac{r}{R_J}\right)^2\right) & \text{if } r < R_J, \\ -\frac{N}{r} & \text{if } r > R_J, \end{cases}$$

where $R_J = N^{1/3} r_S$ is the cluster radius and $V_{\rm JM}$ is the jellium background potential. This model implicitly assumes that the valence electrons are well separated from the core electrons. Since there is a large overlap between $5s$ and $4d$ electron wave functions in Ag atom, the jellium model for silver clusters needs to be modified. The assumption underlying the present model is that the jellium background is no longer rigid but polarizable. Any delocalized $5s$ electron induces a dipole into the jellium core which in turn interacts with another $5s$ electron; thus core polarization leads to the addition to the above Hamiltonian of both a one-body potential $V_{\rm cp}$ and a two-body interaction $u_{\rm cp}$; see the Appendix for the derivation of these polarization terms entering the polarization-corrected jellium Hamiltonian:

$$H = \sum_i \left(-\frac{1}{2}\nabla_i^2\right) + \sum_i V_{\rm JM}(\mathbf{r}_i) + \sum_i V_{\rm cp}(\mathbf{r}_i) + \sum_{i<j} \frac{1}{|\mathbf{r}_i - \mathbf{r}_j|} + \sum_{i<j} u_{\rm cp}(\mathbf{r}_i, \mathbf{r}_j). \qquad (4)$$

The relevant parameter to measure the strength of both core-polarization terms is the dipole polarizability of the Ag^+ ions that constitute the jellium core. Relativistic RPAE calculations for free silver cations predict a value $\alpha_d^f = 8.82a_0^3$ [39]. However, one needs to estimate the polarizability of a Ag^+ ion which is embedded into the jellium. Following Refs. [25,26] we add to the central nuclear potential the electrostatic potential associated with a uniformly distributed Wigner-Seitz sphere of one negative charge with the silver density parameter $r_s = 3.02a_0$. Within this model for an embedded ion, our atomic nonrelativistic RPAE calculation gives an embedded polarizability $\alpha_d^e = 11.27a_0^3$.

As argued by Serra and Rubio [24], the polarizability of Ag^+ on the surface of the cluster should be assigned its free ion value. To account for this difference, we separate a surface shell containing N_f ions with free polarizability from the inner bulk containing N_e ions with embedded polarizability. For small clusters Ag_N with $N \leqslant 21$, all the silver ions are considered as staying on the surface. For Ag_{58} and Ag_{59}^+ the number of embedded silver cores is obtained by using the atomic structure given in Ref. [40] with $N_e = 13$. In the same way, for Ag_{138} and Ag_{139}^+ the number of embedded silver ions is 55. For Ag_{198} we assume that the surface shell has the same thickness as that of Ag_{138} to yield $N_e = 89$.

Since our purpose is to investigate small-amplitude dipole vibration modes, we need to consider in the linear response only the dipole term of the multipole decomposition of the residual interaction. Actually, other multipoles contribute to the RPAE matrix elements defined below in Eqs. (13)–(15); they are fully taken into account in the Coulomb interaction but neglected in the core-polarization residual interaction because they are much smaller. Within these assumptions and as can be seen in the Appendix, the two-body core-polarization dipole interaction is separable and can be written as

$$u_{\rm cp}(\mathbf{r}_i,\mathbf{r}_j) = -N\alpha f(\mathbf{r_i}) f(\mathbf{r_j}), \tag{5}$$

where $N\alpha = N_f\alpha_d^f + N_e\alpha_d^e$ and the interaction form factor is

$$f(\mathbf{r}) = \begin{cases} \frac{\mathbf{r}}{R_J^3} & \text{if } r < R_J, \\ \frac{\mathbf{r}}{r^3} & \text{if } r > R_J, \end{cases}$$

while the one-body term reads

$$V_{\rm cp}(\mathbf{r}) = -\tfrac{1}{2}N\alpha f^2(\mathbf{r}). \tag{6}$$

The many-body Hamiltonian of Eq. (4) is separated into a model independent-particle Hamiltonian H_0 and the residual two-body interaction V_r:

$$H = H_0 + V_r, \tag{7}$$

where

$$H_0 = \sum_i^N h_0(\mathbf{r_i}), \tag{8}$$

$$h_0(\mathbf{r}) = -\tfrac{1}{2}\nabla^2 + V_{\rm JM}(\mathbf{r}) + V_{\rm cp}(\mathbf{r}) + U(\mathbf{r}), \tag{9}$$

$$V_r = \frac{1}{2}\sum_{i,j}\left[\frac{1}{|\mathbf{r}_i - \mathbf{r}_j|} - N\alpha f(\mathbf{r_i}) f(\mathbf{r_j})\right] - \sum_i U(\mathbf{r_i}). \tag{10}$$

In the present work the potential U is the nonlocal Hartree-Fock (HF) potential as

$$U\phi_a(\mathbf{r}) = -\sum_b \int d\mathbf{r}'\left(\frac{1}{|\mathbf{r}-\mathbf{r}'|} - N\alpha f(\mathbf{r}) f(\mathbf{r}')\right) \times [\phi_b^\dagger(\mathbf{r}')\phi_b(\mathbf{r}')\phi_a(\mathbf{r}) - \phi_b^\dagger(\mathbf{r}')\phi_a(\mathbf{r}')\phi_b(\mathbf{r})], \tag{11}$$

where the ϕ's are the single-particle wave functions and the summation extends over occupied states. Restricting to closed-shell systems, we are led to solve radial HF equations for the occupied orbitals. The next step is to construct the many-body dipole modes, which is done by solving the RPAE matrix equation

$$\begin{pmatrix} A & B \\ B^* & A^* \end{pmatrix}\begin{pmatrix} X^k \\ Y^k \end{pmatrix} = \omega^k \begin{pmatrix} X^k \\ -Y^k \end{pmatrix}. \tag{12}$$

The matrix A contains matrix elements of the Coulomb plus core-polarization interaction between particle-hole excitations, whereas the matrix B is composed of matrix elements of that interaction between the ground state and two-particle–two-hole excitations:

$$A_{ma,nb} = (\varepsilon_m - \varepsilon_a)\delta_{ab}\delta_{mn} + \langle mb|V_r|an\rangle, \tag{13}$$

$$B_{ma,nb} = \langle mn|V_r|ab\rangle, \tag{14}$$

$$\langle ij|V_r|kl\rangle = \left\langle ij\left|\frac{1}{|\mathbf{r}-\mathbf{r}'|} - N\alpha f(\mathbf{r}) f(\mathbf{r}')\right|kl\right\rangle - \left\langle ij\left|\frac{1}{|\mathbf{r}-\mathbf{r}'|} - N\alpha f(\mathbf{r}) f(\mathbf{r}')\right|lk\right\rangle. \tag{15}$$

The indices a,b (n,m) refer to the hole (particle) states. The positive eigenvalues ω_k of Eq. (12) are the excitation energies of the system. The corresponding eigenvectors representing the physical states are linear combinations of the forward-going and backward-going amplitudes X_{ma}^k and Y_{ma}^k that satisfy the normalization equation

$$\sum_{a,m}\left(|X_{ma}^k|^2 - |Y_{ma}^k|^2\right) = 1. \tag{16}$$

The dipole transition amplitude from the ground state to the kth excited state is expressed in terms of reduced matrix elements of the dipole operator d as

$$q_k = \sum_{a,m}\left(X_{ma}^k - Y_{ma}^k\right)\langle\phi_m||d||\phi_a\rangle, \tag{17}$$

and the corresponding oscillator strength is given by

$$f_k = \tfrac{4}{3}\omega_k q_k^2. \tag{18}$$

The numerical solution of the eigenvalue problem follows exactly the procedure used in Ref. [37] where the needed complete set of single-article states is obtained by confining the cluster in a large cavity and expanding the HF orbitals in terms of a finite number of B splines. The accuracy of the method can be checked by the Thomas-Reiche-Kuhn f sum rule $\sum_k f_k = N$ being satisfied to better than one part in 10^4. The theory produces a discrete spectrum of oscillator strengths f_k from which one can express the photoabsorption

cross section

$$\sigma(E) = 2\pi^2 \frac{e^2\hbar}{mc} \sum_k f_k \delta(E - \hbar\omega_k). \tag{19}$$

III. RESULTS AND DISCUSSION

In the present paper we shall consider only free silver clusters in vacuum, notwithstanding that most of the experiments have been performed with clusters embedded into a weakly interacting rare-gas matrix [41–43] or deposited on a surface [44,45]. The effect of the surrounding medium will be discussed in a subsequent paper.

Tiggesbäumker *et al.* [19,20] published high-quality photofragmentation cross sections of free Ag clusters Ag_9^+, Ag_{21}^+, $Ag_{50\pm3}^+$, and $Ag_{70\pm5}^+$ using ion beam deletion spectroscopy. These data which precisely reflect photoabsorption cross sections are shown in Fig. 1. Ag_9^+ and Ag_{21}^+ are closed-shell clusters with 8 and 20 delocalized, respectively, as evidenced experimentally both by the observed single resonance of Lorentzian shape and ionization potential measurements [46]. As our model assumes that clusters are spherical, only closed-shell systems are considered and the experimental data of $Ag_{50\pm3}^+$ will be compared with our prediction for Ag_{58}^+ properly rescaled.

To compare with experimental absorption spectrum results, we make a Lorentzian shape convolution for the oscillator strength such as

$$f_k = \frac{f_k}{\pi} \frac{\gamma}{\gamma^2 + (E - \omega_k)^2}, \tag{20}$$

namely, we replace each line by a Lorentzian distribution of arbitrarily fixed width $\gamma = 0.065\omega_k$. As shown in Fig. 1, the theoretical and experimental photoabsorption spectra of Ag_9^+ and Ag_{21}^+ are in excellent agreement both as to the position of the resonances and the absolute value of the cross section; however, the absolute cross sections are measured within un uncertainty of about 50%. The theoretical spectrum of Ag_{59}^+ is rescaled to compare with the experimental spectrum of $Ag_{50\pm3}^+$ and a good agreement is observed too.

Figure 2 shows that the present theoretical predictions agree nicely with the experimental photodestruction (interpreted as photoabsorption) spectra of closed-shell negatively charged clusters (Ag_7^- and Ag_{19}^-) [21]. However, whereas the peak positions are in excellent agreement, the model yields a broadening of the optical absorption spectrum larger than experimentally measured, which we explain as a limitation

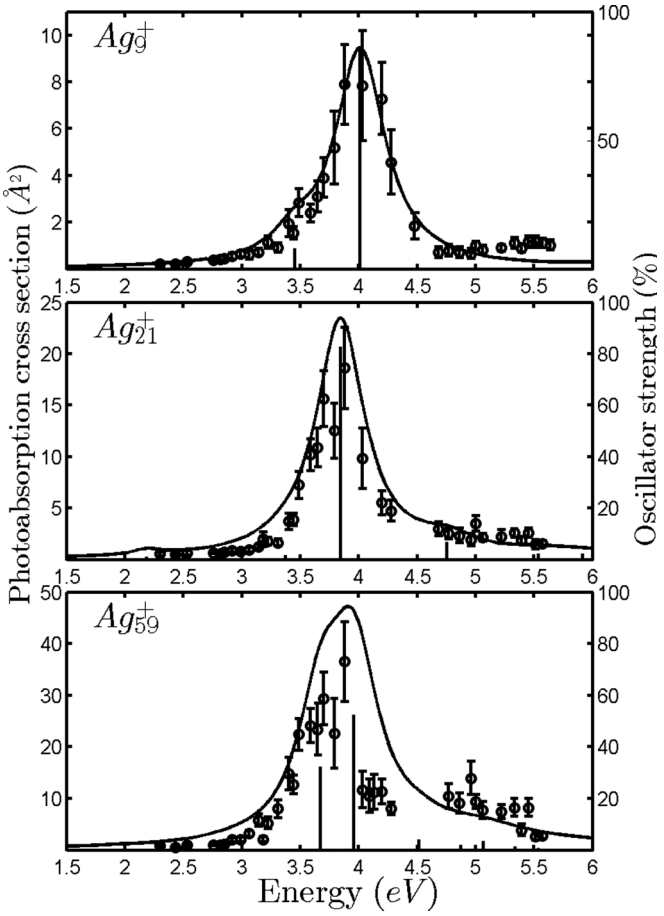

FIG. 1. Photoabsorption cross section ($Å^2$) of free cationic silver clusters as function of dipole transition energy (eV). The scattered circles with error bars are experiment results [20]. The solid vertical lines give the discrete oscillator strength distribution calculated by RPAE with the core-polarization-modified jellium model. The continuous line is a Lorentzian shape convolution ($\gamma = 0.065\omega_k$) of the oscillator strength distribution. Note that the Lorentzian shape convolution of Ag_{59}^+ is rescaled by a factor of 50/58 to compare with experimental data for $Ag_{50\pm3}^+$.

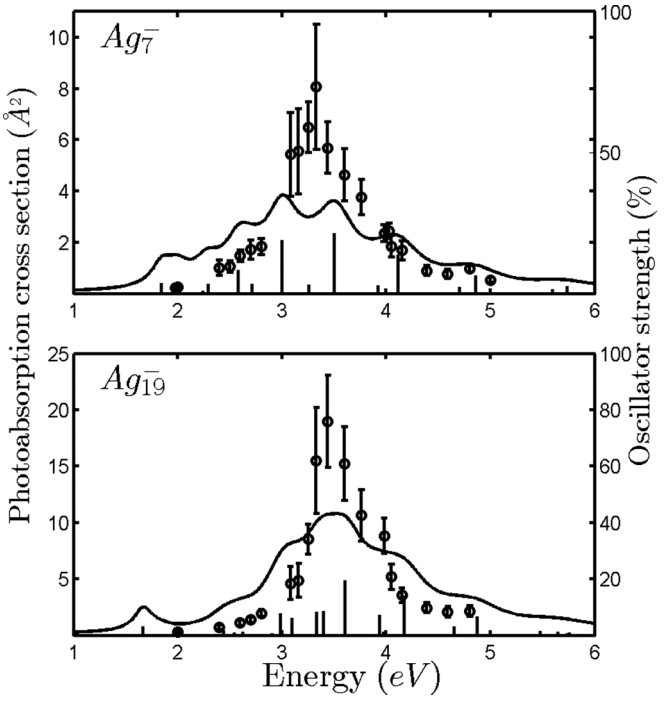

FIG. 2. Photoabsorption cross section ($Å^2$) of free anionic silver clusters as a function of dipole transition energy (eV). The scattered circles with error bars are experiment results [21]. The solid vertical lines give the discrete oscillator strength distribution calculated by RPAE with the core-polarization-modified jellium model. The continuous line is a Lorentzian shape convolution ($\gamma = 0.065\omega_k$) of the oscillator strength distribution.

of the jellium assumption. Indeed the model assumes no relaxation of the ionic core distribution to adjust to the excess electron. Consequently the larger fragmentation of the collective dipole excitation which is expected from the larger spill out as compared with a neutral or cationic cluster is possibly overestimated. One sees that polarizable jellium RPAE model is able to explain the observed trends for the few data available. The theoretical predictions can be understood qualitatively as follows. The main contribution to the dipole strength redistribution arises from the the dipole component of the residual interaction which contains the Coulomb term and the core-polarization term:

$$V_r^{L=1}(\mathbf{r},\mathbf{r}') = \left(\frac{r_<}{r_>^2} - N\alpha f(r) f(r')\right)\cos(\theta_{\mathbf{r},\mathbf{r}'}), \qquad (21)$$

where $r_<$ and $r_>$ are the smallest and largest of the two electron radial positions. It can be written as

$$V_r^{L=1} = \beta V_{\text{Coulomb}}^{L=1}. \qquad (22)$$

where the screening factor β is

$$\beta = 1 - \frac{\alpha}{r_s^3} R_J^3 \frac{r_>^2}{r_<} f(r_<) f(r_>). \qquad (23)$$

As the dipole transition density is peaked at the surface, one can write down the following approximations:

$$\beta \approx \begin{cases} 1 - \frac{\alpha}{r_s^3}\frac{R_J^3}{r_<^3} & \text{if } R_J < r_<, \\ 1 - \frac{\alpha}{r_s^3} & \text{if } r_< < R_J < r_>, \\ 1 - \frac{\alpha}{r_s^3}\frac{r_>^3}{R_J^3} & \text{if } r_> < R_J. \end{cases}$$

In the large size limit, the effective screened electron charge is about $e^* = \sqrt{1 - \frac{\alpha}{r_s^3}}$ which in the Drude model would lead to a red shift of the Mie resonance [Eq. (1)] from 5.2 to 3.9 eV to compare with the empirical value of 3.5 eV [Eq. (2)]. In this limit, the one-body core-polarization potential of Eq. (6) does not contribute. However, it has a size dependence which yields a blue shift of the plasmon frequency with decreasing cluster size. This is readily seen as the attractive jellium background potential is strengthened in the surface region and consequently the Mie frequency of Eq. (1) is blue shifted by a size-dependent multiplying factor of about $(1 + \frac{\alpha}{2Nr_s^3})$. Moreover, the increasing fraction of lower surface polarizability as discussed in previous papers [20,24] also contributes to this blue shift.

However, the size-dependent blue shift arising from one-body core polarization is competing with the size-dependent red shift due to electron spill out. This competition leads to an overall size dependence which changes sign as the total electrical charge of silver clusters changes from positive to negative. In cationic clusters with an extra positive charge in the jellium background, the relatively weak electron spill out cannot beat the core-polarization effect, and the overall size dependence predicted by the model and observed experimentally is a blue shift, see Figs. 3 and 6. In anionic clusters with an extra negative charge in the jellium background, the relatively large electron spill out beats the core-polarization effect, and the overall size dependence predicted by the model and observed experimentally is a red shift, see Figs. 4 and 6.

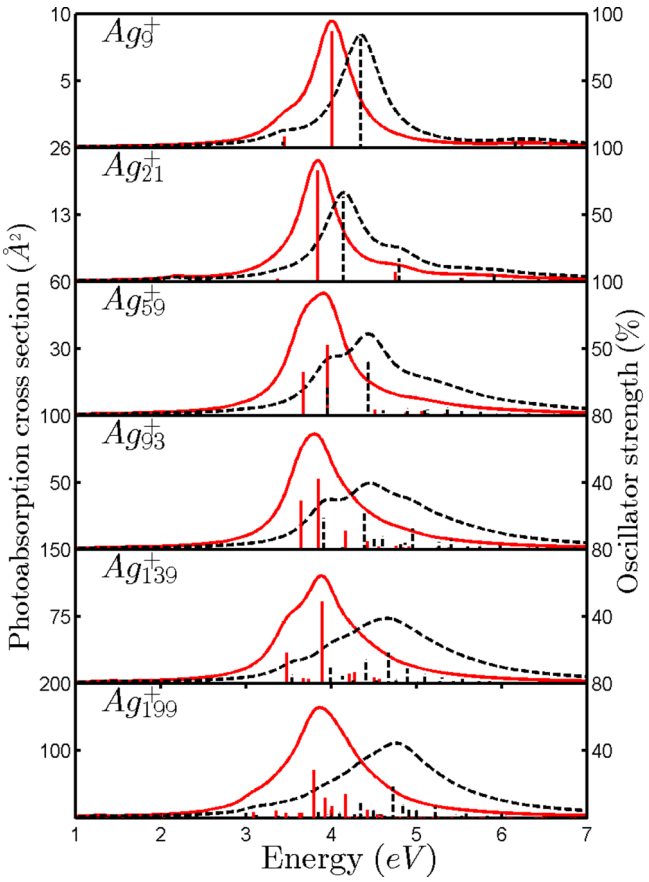

FIG. 3. Photoabsorption cross section ($Å^2$) of free cationic silver clusters as a function of dipole transition energy (eV). Dashed vertical lines are oscillator strengths calculated by RPAE within a pure jellium model. Red solid vertical lines are oscillator strengths calculated by RPAE within a core-polarization-modified jellium model. The continuous solid and dashed lines are Lorentzian shape convolutions ($\gamma = 0.065\omega_k$) of the corresponding oscillator strength distributions.

For neutral clusters the competition between electron spill out and core polarization is more balanced leading to an slightly red-shifted size-dependent surface plasmon frequency, as shown in Fig. 5. Let us recall that there are no experimental data on free neutral clusters and the experimentally observed blue shifts concern silver clusters placed on a substrate for which the effects of the latter need to be considered [44,45,47].

IV. CONCLUSION

The average dipole vibration mode of small closed-shell silver clusters (assuming that 5*s* electrons are fully delocalized) can be nicely described by a random-phase approximation with exact exchange (equivalent to a time-dependent Hartree-Fock model) within a polarizable jellium model. The polarizability of the jellium core implies that the jellium Hamiltonian needs to be modified both in the one-body potential and in the two-body electron-electron interaction. Jellium core polarization leads to a screening of dipole component of the Coulomb interaction in both the direct and exchange terms. The only parameter which enters the present model

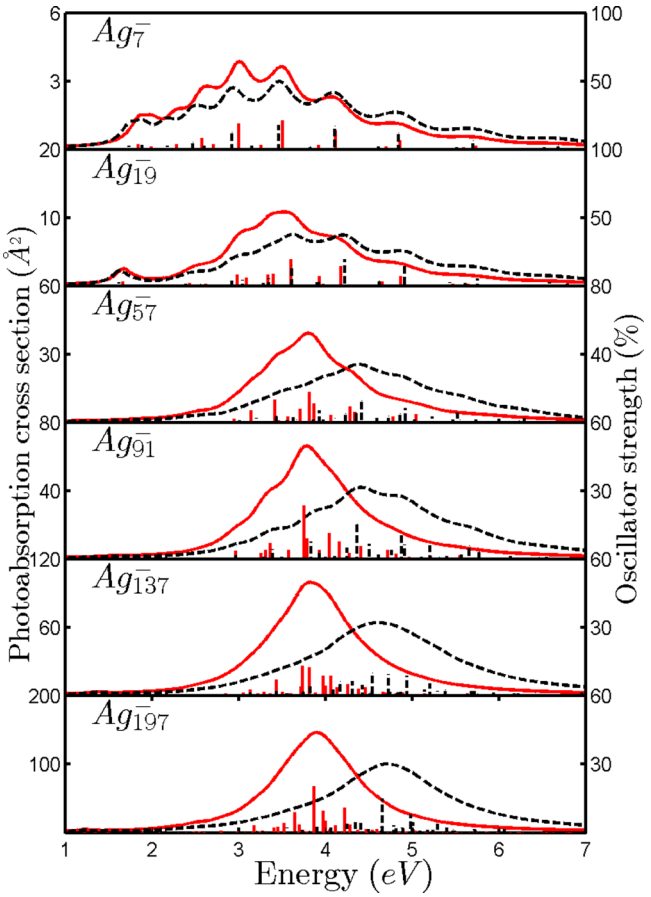

FIG. 4. Same as Fig. 3, but for free anionic silver clusters.

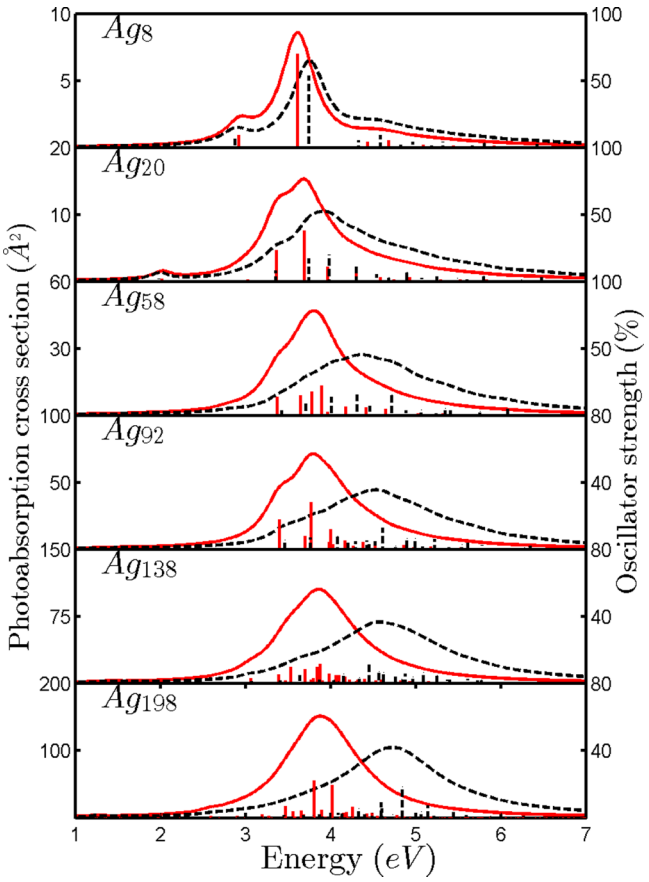

FIG. 5. Same as Fig. 3, but for free neutral silver clusters.

is the dipole polarizability of silver cations that constitute the jellium; this parameter can be calculated in a fully independent atomic model. The red and blue shifts of the surface plasmon peak as the cluster size varies, which has been extensively discussed in the literature results from a subtle interplay between core-polarization screening and spill-out effect. The present model explains well the observed blue shift with decreasing cluster size for cationic silver clusters as well as the red shift for anionic clusters. The next challenge will be to adapt a jellium approach for gold clusters where relativistic effects are important. It should be borne in mind that the present approach does not claim to compete with full *ab initio* calculations such as real time TDDFT, but to provide an insight on the dominating phenomena that control the physics under study; it has the advantage of allowing calculations for large clusters which are prohibitive for *ab initio* calculations and allowing linkage with classical calculations.

ACKNOWLEDGMENTS

The authors thank J. Tiggesbäumker for sending us experimental data, and S. A. Blundell for fruitful comments and reading through the manuscript. Discussions with Su Haibin are acknowledged.

APPENDIX: JELLIUM POLARIZATION INTERACTION

Let N silver cations and N electrons form a bound system. The electric field $\mathbf{E}(\mathbf{R}_a)$ on the site of a silver cation a located at position $\mathbf{R}_a$, generated by the other silver cations at positions

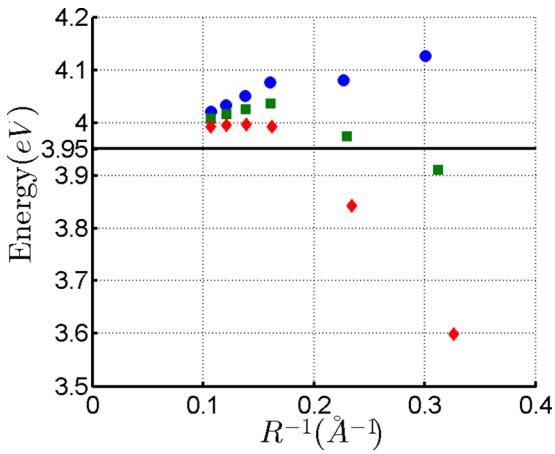

FIG. 6. Theoretical evolution of the surface plasmon peak as a function of the inverse radius of silver clusters: cationic clusters (blue circles), anionic clusters (red diamonds), neutral clusters (green squares). The black line of 3.95 eV shows the large cluster limit predicted by our model.

$\mathbf{R}_j$ and the valence electrons at positions $\mathbf{r}_i$, is

$$\mathbf{E}(\mathbf{R_a}) = \sum_j \frac{\mathbf{R_a} - \mathbf{R}_j}{|\mathbf{R_a} - \mathbf{R}_j|^3} - \sum_i \frac{\mathbf{R_a} - \mathbf{r}_i}{|\mathbf{R_a} - \mathbf{r}_i|^3}. \tag{A1}$$

Let α be the atomic dipole polarizability of a single silver cation. The induced polarization leads to a polarization energy

$$V_p = -\frac{1}{2}\alpha \sum_a |\mathbf{E}(\mathbf{R_a})|^2. \tag{A2}$$

Within the spherical jellium approximation, we average the core-polarization energy over the cation distribution of constant number density n_i as $n_{\rm ion}(\mathbf{R}) = n_i\theta(R_J - |\mathbf{R}|) = \frac{3}{4\pi r_s^3}\theta(R_J - |\mathbf{R}|)$, where $\theta(x)$ is the step function equal to 1 for $x > 0$ and to 0 for $x < 0$ and R_J the jellium radius. This gives

$$V_p = -\frac{1}{2}\alpha n_i \int_0^{R_J} d\mathbf{R} |\mathbf{E}(\mathbf{R})|^2. \tag{A3}$$

Only the part depending on the electron position enters the jellium Hamiltonian [Eq. (4)]. Therefore the core-polarization potential in this Hamiltonian has two terms, namely, a one-electron term $V_{\rm cp}$ and a two-electron term $u_{\rm cp}$. Expanding Eq. (A2), the one-body term reads

$$V_{\rm cp}(\mathbf{r}_i) = \frac{1}{2}\alpha n_i \int_0^{R_J} d\mathbf{R} \sum_I 2\frac{\mathbf{R} - \mathbf{R}_I}{|\mathbf{R} - \mathbf{R}_I|^3}\frac{\mathbf{R} - \mathbf{r}_i}{|\mathbf{R} - \mathbf{r}_i|^3} - \left(\frac{\mathbf{R} - \mathbf{r}_i}{|\mathbf{R} - \mathbf{r}_i|^3}\right)^2, \tag{A4}$$

and the two-body term as

$$u_{\rm cp}(\mathbf{r}_i, \mathbf{r}_j) = -\alpha n_i \int_0^{R_J} d\mathbf{R} \frac{\mathbf{R} - \mathbf{r}_i}{|\mathbf{R} - \mathbf{r}_i|^3}\frac{\mathbf{R} - \mathbf{r}_j}{|\mathbf{R} - \mathbf{r}_j|^3}. \tag{A5}$$

Dealing with dipole transitions only, we only pick up the dipole component of the core-polarization two-body interaction. Other multipoles may contribute to the exchange RPAE matrix elements but they are much smaller and can be neglected with regard to the set of approximations underlying the jellium approximation. Expanding the functions $\frac{1}{|\mathbf{R}-\mathbf{r}|}$ in Legendre polynomials, it is clearly seen that the dipole term reduces to

$$u_{\rm cp}^{L=1}(\mathbf{r}_i, \mathbf{r}_j) \approx -\alpha n_i \int_0^{R_J} d\mathbf{R} \frac{\mathbf{r}_i \cdot \mathbf{r}_j}{r_{>i}^3 r_{>j}^3} \approx -\alpha N \frac{\mathbf{r}_i \cdot \mathbf{r}_j}{r_{>i}^3 r_{>j}^3}, \tag{A6}$$

where $r_{>i}$ denotes the largest of r_i and R_J as explicit in Eq. (5).

As for the one-body potential of Eq. (A4), which enters the jellium Hamiltonian, we need to retain the monopole leading contribution only; it clearly is

$$V_{\rm cp}^{L=0}(\mathbf{r}_i) = -\frac{1}{2}\alpha n_i \int_0^{R_J} d\mathbf{R} \frac{r_i^2}{r_{>i}^6} = -\frac{1}{2}\alpha N \frac{r_i^2}{r_{>i}^6}. \tag{A7}$$

[1] W. D. Knight, K. Clemenger, W. A. de Heer, W. A. Saunders, M. Y. Chou, and M. L. Cohen, Phys. Rev. Lett. **52**, 2141 (1984).
[2] W. D. Knight, K. Clemenger, W. A. de Heer, and W. A. Saunders, Phys. Rev. B **31**, 2539 (1985).
[3] M. M. Kappes, M. Schar, U. Rothlisberger, C. Yeretzian, and E. Schumacher, Chem. Phys. Lett. **143**, 251 (1988).
[4] C. Brechignac, P. Cahuzac, F. Carlier, and J. Leygnier, Phys. Rev. Lett. **63**, 1368 (1989).
[5] K. Selby, M. Vollmer, J. Masui, V. Kresin, W. A. de Heer, and W. D. Knight, Phys. Rev. B **40**, 5417 (1989).
[6] K. Selby, V. Kresin, J. Masui, M. Vollmer, W. A. de Heer, A. Scheidemann, and W. D. Knight, Phys. Rev. B **43**, 4565 (1991).
[7] M. L. Homer, J. L. Persson, E. C. Honea, and R. L. Whetten, Z. Phys. D **22**, 441 (1991).
[8] P. Dugourd, D. Rayane, P. Labastie, B. Vezin, J. Chevaleyre, and M. Broyer, Chem. Phys. Lett. **197**, 433 (1992).
[9] W. A. de Heer, Rev. Mod. Phys. **65**, 611 (1993).
[10] M. Brack, Rev. Mod. Phys. **65**, 677 (1993).
[11] D. E. Beck, Phys. Rev. B **30**, 6935 (1984).
[12] W. Ekardt, Phys. Rev. B **29**, 1558 (1984).
[13] W. Ekardt, Phys. Rev. Lett. **52**, 1925 (1984).
[14] W. Kohn, Phys. Rev. **123**, 1242 (1961).
[15] J. F. Dobson, Phys. Rev. Lett. **73**, 2244 (1994).
[16] L. G. Gerchikov, C. Guet, and A. N. Ipatov, Phys. Rev. A **66**, 053202 (2002).
[17] S. A. Blundell and C. Guet, Z. Phys. D **33**, 153 (1995).
[18] A. Liebsch, Phys. Rev. Lett. **71**, 145 (1993).
[19] J. Tiggesbaumker, L. Koller, H. O. Lutz, and K.-H. Meiwes-Broer, Chem. Phys. Lett. **190**, 42 (1992).
[20] J. Tiggesbaumker, L. Koller, K.-H. Meiwes-Broer, and A. Liebsch, Phys. Rev. A **48**, R1749 (1993).
[21] J. Tiggesbaumker, L. Koller, and K.-H. Meiwes-Broer, Chem. Phys. Lett. **260**, 428 (1996).
[22] V. V. Kresin, Phys. Rev. B **51**, 1844 (1995).
[23] E. Cottancin, G. Celep, J. Lermé, M. Pellarin, J. R. Huntzinger, J. L. Vialle, and M. Broyer, Theor. Chem. Acc. **116**, 514 (2006).
[24] L. Serra and A. Rubio, Phys. Rev. Lett. **78**, 1428 (1997).
[25] K. Sturm, E. Zaremba, and K. Nuroh, Phys. Rev. B **42**, 6973 (1990).
[26] E. Zaremba and K. Sturm, Phys. Rev. Lett. **55**, 750 (1985).
[27] K. Baishya, J. C. Idrobo, S. Ogut, M. Yang, K. Jackson, and J. Jellinek, Phys. Rev. B **78**, 075439 (2008).
[28] C. M. Aikens, S. Li, and G. C. Schatz, J. Phys. Chem. C **112**, 11272 (2008).
[29] M. Harb, F. Rabilloud, D. Simon, A. Rydlo, S. Lecoultre, F. Conus, V. Rodrigues, and C. Felix, J. Chem. Phys. **129**, 194108 (2008).
[30] A. Zangwill and P. Soven, Phys. Rev. A **21**, 1561 (1980).
[31] W. Ekardt, Phys. Rev. B **31**, 6360 (1985).
[32] C. Yannouleas, E. Vigezzi, and R. A. Broglia, Phys. Rev. B **47**, 9849 (1993).
[33] G. Bertsch and R. Broglia, *Oscillations in Finite Quantum Systems* (Cambridge University, New York, 1994).
[34] K. Yabana and G. F. Bertsch, Phys. Rev. B **54**, 4484 (1996).

[35] D. J. Rowe, Rev. Mod. Phys. **40**, 153 (1968).
[36] M. Amusia and N. Cherepkov, Case Stud. At. Phys. **5**, 47 (1975).
[37] C. Guet and W. R. Johnson, Phys. Rev. B **45**, 11283 (1992).
[38] M. Madjet, C. Guet, and W. R. Johnson, Phys. Rev. A **51**, 1327 (1995).
[39] W. R. Johnson, D. Kolb, and K. Huang, At. Data Nucl. Data Tables **28**, 333 (1983).
[40] J. C. Idrobo and S. T. Pantelides, Phys. Rev. B **82**, 085420 (2010).
[41] T. Diederich, J. Tiggesbaumker, and K.-H. Meiwes-Broer, J. Chem. Phys. **116**, 3263 (2002).
[42] S. Lecoultre, A. Rydlo, J. Buttet, C. Felix, S. Gilb, and W. Harbich, J. Chem. Phys. **134**, 184504 (2011).
[43] S. Fedrigo, W. Harbich, and J. Buttet, Phys. Rev. B **47**, 10706 (1993).
[44] J. A. Scholl, A. L. Koh, and J. A. Dionne, Nature **483**, 421 (2012).
[45] S. Raza, N. Stenger, S. Kadkhodazadeh, S. V. Fischer, N. Kostesha, A. P. Jauho, A. Burrows, M. Wubs, and N. A. Mortensen, Nanophotonics **2**, 131 (2013).
[46] C. Jackschath, I. Rabin, and W. Schulze, Z. Phys. D **22**, 517 (1992).
[47] H. Haberland, Nature **494**, E1 (2013).